








Open Archive Toulouse Archive Ouverte

OATAO is an open access repository that collects the work of Toulouse researchers and makes it freely available over the web where possible

This is an author's version published in: <http://oatao.univ-toulouse.fr/21069>

Official URL: <https://doi.org/10.1002/ceat.201800063>

To cite this version:

Malafosse, Claire  and Blanco, Jean-François  and Le Sauze, Nathalie  and Loubière, Karine  and Ollagnier, Jean-Noël and Rolland, Hervé and Pierre, Aurélie and Prat, Laurent E.  *Effects of Process Parameters on an Inverse Concentrated Miniemulsion Flowing in a Microchannel*. (2018) *Chemical Engineering and Technology*, 41 (10). 1965-1974. ISSN 0930-7516

Any correspondence concerning this service should be sent to the repository administrator: tech-oatao@listes-diff.inp-toulouse.fr

Claire Malafosse¹
Jean-François Blanco¹
Nathalie le Sauze¹
Karine Loubière¹
Jean-Noël Ollagnier²
Hervé Rolland²
Aurélie Pierre³
Laurent Prat^{1,*}

Effects of Process Parameters on an Inverse Concentrated Miniemulsion Flowing in a Microchannel

Emulsions are of great industrial interest due to their wide variety and end-use properties. Microfluidics systems provide excellent control of transport phenomena. Hence, the influence of operating parameters on a concentrated inverse miniemulsion flowing in a microfluidic system was investigated. The feasibility of maintaining the emulsion in a microfluidic device was clearly demonstrated and the associated operating domain identified. Due to its influence on rheology, the effect of temperature on the droplet size distribution was quantified. Under specific conditions, a mass transfer phenomenon between the train of water drops and the smallest droplets of the emulsion was found, potentially explained by a difference in osmotic pressure between the two aqueous phases.

Keywords: Inverse miniemulsions, Microfluidic systems, Process parameters, Stability

1 Introduction

Emulsions are widely used in industry and are a part of many different products. There are numerous examples in the pharmaceutical, agricultural, and food industries in which emulsions play an important role. In the case of biphasic reactive systems such as nitration, transesterification, and polymerization, the droplet size distribution and the mean diameter are the key parameters to control the efficiency of the mass transfer between phases, the reaction performance, and the final properties of the product [1–3].

Emulsions are thermodynamically unstable systems. The operating conditions to which they are subjected, in particular those found in large scale industrial processes, may promote various phenomena leading to their destabilization, such as coalescence, flocculation, creaming, sedimentation, phase inversion, and Ostwald ripening [4,5]. Dispersed phase fraction, temperature, and hydrodynamic conditions are some of the parameters influencing the droplet size distribution [6,7]. Depending on the targeted size and the stability time required, surfactants are often added (1) to facilitate dispersion by lowering the interfacial tension and inhibiting coalescence during the emulsification step and (2) to stabilize the dispersion by alleviating the degradation phenomena. The optimum concentration of surfactant to stabilize the emulsion may be around the critical micelle concentration [8], but specific formulations with higher concentrations may be developed in industrial contexts [9]. The more conventional devices used on an industrial scale to produce emulsions at present are high pressure homogenizers, colloid mills, static mixers, and stirred tanks [10,11]. All of them require a given energy input to disperse the two phases. The energy dissipated per unit volume, which is the

parameter generally used, can be high depending on the targeted size and on the applied technology, e.g., up to 10^6 J m^{-3} in colloid mills [12] or 10^8 J m^{-3} in high pressure homogenizers [13].

Liquid liquid reactions are often performed in stirred tanks operating in continuous or batch mode, which remain the most widely used technology on an industrial scale. However, the hydrodynamic and temperature conditions are often inhomogeneous in this type of equipment, and this restricts the development of processes and formulations with very high content of dispersed phase. Indeed, the local heterogeneities inherent to this type of technology may generate local destabilization of the emulsion and do not allow perfect control of the end use properties of the targeted products. It is then interesting, in particular when faced with reactive media involving highly concentrated emulsions, to propose new reactors in which homogeneous mixing and high mass/heat transfer efficiencies can be achieved. To optimize these new reactors, the limiting phenomena involved in the reaction step must first be determined.

From this perspective, microfluidic systems have emerged in the last decades as relevant technologies for reaction intensifi

¹Claire Malafosse, Jean François Blanco, Nathalie le Sauze, Karine Loubière, Prof. Laurent Prat
Laurent.prat@ensiacet.fr
Laboratoire de Génie Chimique, Université de Toulouse, CNRS, INPT, UPS, 4 allée Emile Monso, CS84234, 31432 Toulouse, France.

²Jean Noel Ollagnier, Hervé Rolland
SEPPIC, Air Liquide, 127 chemin de la Poudrerie BP 90228, Castres, 81105, France.

³Aurélie Pierre
SEPPIC, Air Liquide, 22 Terrasse Bellini Paris La Défense, Puteaux, 92800, France.

cation. The small size of microreactors increases the specific exchange areas and decreases the characteristic lengths to promote excellent control of temperature and extensive mass transfer [14, 15]. The hydrodynamics in microfluidic reactors is well controlled and the structures generated are favorable to mass transfer in liquid liquid systems [16]. It thus presents new possibilities in chemical synthesis for implementing fast and exothermic reactions, in particular those involving emulsions.

The present work aimed to investigate the evolution of the characteristics of a concentrated inverse miniemulsion flowing in a spatially confined microfluidic system at temperatures up to 80 °C. In particular, concentrated inverse emulsions, which are a particular case of emulsions characterized by an organic continuous phase with a concentration lower than 35 vol% and droplet size between 0.1 and 1 μm, were considered. This kind of emulsions is present in a large range of products, from paints [17] to cosmetics [18, 19], and the characterization and control of their physical properties throughout the fabrication process are of great interest. In the field of polymerization, miniemulsions make it possible to synthesize complex materials that cannot be produced otherwise, including adhesives, textile pigments, and drug delivery systems [20]. They allow easier control of polymer characteristics due to the dependence of the polymer size on the droplet size. When implementing such polymerization reactions, the characteristic size of the miniemulsion tends to prevent reversible destabilization phenomenon due to weak gravitational forces and Brownian motion [21]. Moreover the apparent viscosity of an inverse emulsion is independent of the conversion, and this favors the implementation of the reaction.

Even though there are many references to microfluidic devices for making emulsions, few articles were interested in studying the evolution of the characteristics of a concentrated inverse emulsion flowing in this type of apparatus, and in particular under the influence of significant temperatures. Moreover, when carrying out reactions involving such emulsions, the first step consists of introducing a reagent into the dispersed phase. This configuration, i.e., the introduction of a secondary flow into an emulsion, is characterized by the occurrence of mass transfers between this flow and the two phases forming the emulsion, and has so far not been discussed in the literature, especially when performed in a microfluidic system.

The main objective of this study was thus to define a range of process parameters allowing implementation of a reactive concentrated inverse miniemulsion in a microfluidic system while preserving the initial properties of the emulsion. The tracking of the emulsion characteristics according to the flow conditions as well as the understanding and control of the exchanges involved between the secondary flow and the emulsion are a preliminary step to identify the operating domain that ensures the stability of the emulsion.

First, the studied emulsion, the microfluidic systems, and the protocols are presented. This part covers (1) the design of the microfluidic system, in particular when a secondary flow is added in a coflow configuration, (2) the process parameters imposed, such as shear rate, temperature, and residence time, and their measurement, (3) the set of methods developed to analyze these multiphase systems at different scales, which

combines measurement of nanometric droplet size, characterization of rheological behavior, and imaging.

Second, the influence of the hydrodynamic conditions and temperature on the droplet size distribution and mean diameter of the emulsion flowing alone in a microchannel was studied. Special attention was paid to uncoupling the phenomena induced by the spatial confinement and by the temperature.

Third, the addition of an aqueous flow in an oil phase by means of a coflow configuration allowed the hydrodynamic behavior of this phase in the phase constituting the continuous medium of the emulsion to be described. Fourth, the consequences of adding an aqueous secondary flow for the emulsion characteristics was investigated. Finally, global analysis of the system and conclusions are presented.

2 Materials and Methods

2.1 Description of the Emulsion

A 66 vol% water in oil miniemulsion was considered in this study. The continuous phase of this emulsion was a mineral oil with 10 wt% of a nonionic surfactant with low hydrophilic lipophilic balance (HLB) between 1 and 6, namely, a sorbitan ester. This concentration of surfactant was largely above the critical micelle concentration, which was measured to $3.6 \times 10^{-4} \text{ mol L}^{-1}$ (0.06 wt%) at 20 °C. Such conditions were chosen in accordance with the industrial conditions. According to technical data, the density of the oil was 790 kg m^{-3} . The dispersed phase was composed of a commercial solution of ethylenic monomer, electrically neutral, anionic, or cationic, at 55 wt% in water. The inverse emulsion was prepared at laboratory scale in a 250 mL vessel. The aqueous solution was added to the oil solution with moderate mixing and the emulsion was prepared by using an ULTRA TURRAX rotor stator (IKA WERK) at approximately 6000 rpm for 2 min. The density of the emulsion was estimated to be about 1070 kg m^{-3} at ambient temperature.

In the coflow configurations, the dispersed phase was water, and two standard continuous phases were studied, corresponding either to the oil used in the emulsion or to a solution of 10 wt% of surfactant in oil, i.e., the composition of the continuous phase of the emulsion. Finally, the coflow was performed with water flowing in the emulsion described above.

A cone and plane rheometer (AR 2000 EX, TA Instruments) was used to measure the rheological behavior of the emulsion and the oil.

It was observed (Appendix A) that the emulsion had a shear thinning behavior that could be globally described by a power law [Eq. (1)] in the range of $1 - 100 \text{ s}^{-1}$, regardless of the temperature level. This range of shear rates $\dot{\gamma}^{(1)}$ corresponds to those applied in the microchannel, which range from 2 to 71 s^{-1} depending on the flow rate and temperature (Tab. 1; see Appendix B for explanation of calculation).

$$\mu(\dot{\gamma}) = k(T)\dot{\gamma}^{n(T)-1} \quad (1)$$

1) List of symbols at the end of the paper.

Table 1. Mean shear rates in the microchannel under different operating conditions.

D [mm]	Q_t [mL h ⁻¹]	T [°C]	$\langle \dot{\gamma} \rangle$ [s ⁻¹]
1	30	20	33.9
1	30	50	35.4
1	30	65	31.7
1	30	80	31.7
1	7	20	7.9
1	7	50	8.3
1	7	65	7.4
1	7	80	7.4
1	2	20	2.3
1	2	50	2.4
1	2	65	2.1
1	2	80	2.1
0.5	7.3	50	70.8
0.5	5.2	80	48.4
0.5	2.4	20	67.7
0.5	2.7	65	25.1

where μ is the viscosity and k and n , which are the consistency and flow index, were dependent on temperature, as shown in Tab. 2 and in Appendix A.

Table 2. Consistency and flow index of the emulsion depending on temperature (see Appendix A).

T [°C]	k [kg m ⁻¹ s ⁽ⁿ⁻²⁾]	n []
20	3.05	0.48
50	1.13	0.45
65	0.61	0.37

At 20 °C, oil and oil with 10 wt % of surfactant were Newtonian with viscosities of 4.1×10^{-3} and 5.6×10^{-3} Pa s, respectively.

Interfacial and surface tensions were both measured by the Wilhelmy balance method with a GBX 3S tensiometer. At 20 °C surface tensions of the organic phase with or without surfactant and the aqueous phase were 25 and 52 mN m⁻¹ respectively. Whatever the temperature from 20 to 65 °C, interfacial tension between the two phases was less than 2 mN m⁻¹ in the presence of surfactant and

around 20 mN m⁻¹ without surfactant in the oil phase. For this temperature range and in the presence of surfactant, the interfacial tension was around 3 mN m⁻¹ when there was no monomer in the dispersed phase. This would thus suggest that the monomer acts as a co surfactant in this system.

2.2 Microfluidic Setup

To study the influence of the design of the microfluidic system and the process parameters on the evolution of the emulsion characteristics, an adjustable microfluidic system was built (Fig. 1). The reactor consisted of a perfluoroalkoxy alkane (PFA) tubing with 0.5 or 1 mm inner diameter D , 1.59 mm outer diameter, and length L of 1.3 10 m. The tube was rolled around a hollow cylindrical support made of aluminum, through which a coolant fluid flowed from a thermostatic bath (F33 MA Julabo). The temperature was measured at the outer wall of the tube and at half the length by using a Pt 100 surface sensor and was thus slightly higher than the real temperature of the fluid due to the insulating material of the tube.

The emulsion or oil was introduced into the tubing by a high pressure syringe pump (neMESYS). A secondary aqueous flow can be added to the emulsion or to the oil by a second syringe pump, for which a fused silica capillary (Postnova Analytics) of 50 μ m in inner diameter d and 363 μ m in outer diameter was connected to the main tubing. The corresponding ratio of flow rates of disperse and continuous phases Q_d/Q_c should be kept very small in order to maintain the volume fraction of the aqueous phase below 74 vol % and to avoid phase inversion when the continuous phase is an emulsion. For this purpose, a coflow configuration was chosen as being the most suitable to implement such stringent requirements. The neMESYS pump was equipped with stainless steel syringes (Harvard Apparatus). The flow rates that can be implemented are then limited by the pressure supported by the syringes, namely, less than 20 bar.

Three configurations of the setup were specifically considered, as described in Tab. 3. In each case, the effects of temperature and shear rate were investigated.

Setup 1 was devoted to studying the emulsion flowing alone through the microchannel, i.e., in the PFA tube. Two inner

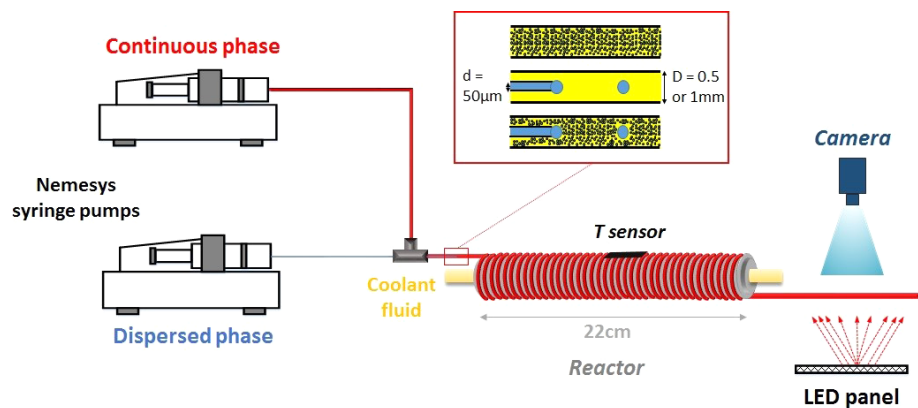
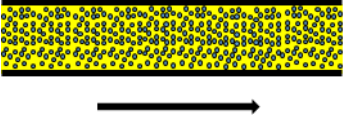

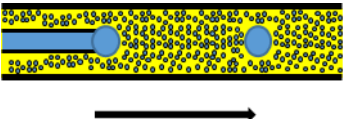


Figure 1. Microreactor setup.

Table 3. Description of the three configurations under test

Setup	Continuous phase	Dispersed phase	Schematic representation Flow
1	Emulsion		
2	Oil	Water	
3	Emulsion	Water	

diameters D of the tube were investigated, 1 and 0.5 mm, in order to enlarge the range of mean shear rates investigated. The flow rates varied from 2 to 30 mL h⁻¹ and the length L was adjusted to reach residence times of 15 or 30 min. The latter was chosen as corresponding to some characteristic reaction times that will be used in the future.

Setup 2 was devoted to a preliminary study in a coflow configuration in which water was the dispersed phase and oil the continuous one. Tubing with $D = 1$ mm was chosen as a good compromise between pressure drop and syringe volume capacity. Experiments were carried out without surfactant in the continuous phase and with 10 wt % of surfactant. Flow rates from 2 to 30 mL h⁻¹ were investigated with flow rate ratios varying from 2 to 10 %.

Setup 3 was a combination of the first two setups. It corresponded to a coflow in which the dispersed and continuous phases were water and the emulsion, respectively. Droplets of water were then generated in the emulsion. The same process parameters as previously were investigated, namely, flow rates between 2 and 30 mL h⁻¹, flow rate ratios between 2 and 10 %, and temperatures between 20 and 80 °C.

2.3 Methods for Characterizing the System

2.3.1 Macroscopic Analysis: Image Analysis

The phenomena occurring in the different setups were characterized at a macroscopic scale by image analysis. Images were recorded at the inlet and outlet of the microchannel by using a camera (sCOMS pco.edge) equipped with a 105 mm f/2.8 lens (Sigma) at a frame rate of 50 fps. Images were processed with ImageJ software. Lighting was furnished by a 24 V LED panel (Phlox gc) as backlight.

2.3.2 Microscopic Analysis: Particle Size Distribution

Microscopic analysis was realized by measuring the evolution of droplet size distribution in the emulsion at the inlet and the outlet of the microchannel, i.e., before and after having been subjected to specific perturbations in terms of shear rates and/or temperature. Samples were collected at the outlet of the microreactor, diluted in a solvent composed of the standard oil and the 10 wt % surfactant, and analyzed by laser diffraction with a Mastersizer 3000 (Malvern). Dilution was performed to obtain an obscuration rate between 3 and

20 % of laser power. These measurements provided the particle size distribution and the Sauter mean diameter defined by Eq. (2). A normalized Sauter mean diameter $d_{3,2N}$ was defined according to the ratio of the Sauter mean diameter at the outlet of the reactor $d_{3,2}$ to that at the inlet $d_{3,2i}$ (Eq. (3)).

$$d_{3,2} = 6 \frac{V_p}{A_p} \quad (2)$$

$$d_{3,2N} = \frac{d_{3,2}}{d_{3,2i}} \quad (3)$$

where V_p and A_p are the volume and surface area of one droplet, respectively. The width of the distribution was described by the full width at half maximum $l_{1/2}$.

3 Results and Discussion

3.1 Characteristics of the Emulsion Flowing Alone in the Microchannel

First, the behavior of the emulsion flowing alone in a microchannel was investigated. The goal was to understand and isolate the effects of spatial confinement, temperature, and the hydrodynamic conditions, such as mean shear rate, on the characteristics of the emulsion.

Fig. 2 a shows the variation of normalized Sauter mean diameter [Eq. (3)] as a function of the mean shear rate at different temperatures, and Fig. 2 b the variation of the volume size distribution of the emulsion depending on the temperature, at 30 mL h⁻¹ in a tube with 1 mm inner diameter. The droplet size increases with increasing temperature. The characteristic size of the emulsion droplets at the outlet of the tube increases from $0.27 \pm 0.03 \mu\text{m}$ at 20 °C to $0.47 \pm 0.06 \mu\text{m}$ at 80 °C. Moreover, the size distribution becomes broader, and $l_{1/2}$ increases from $0.8 \mu\text{m}$ at 20 °C to $3.2 \mu\text{m}$ at 80 °C. However, the particle size distribution still showed some droplets smaller than $0.3 \mu\text{m}$.

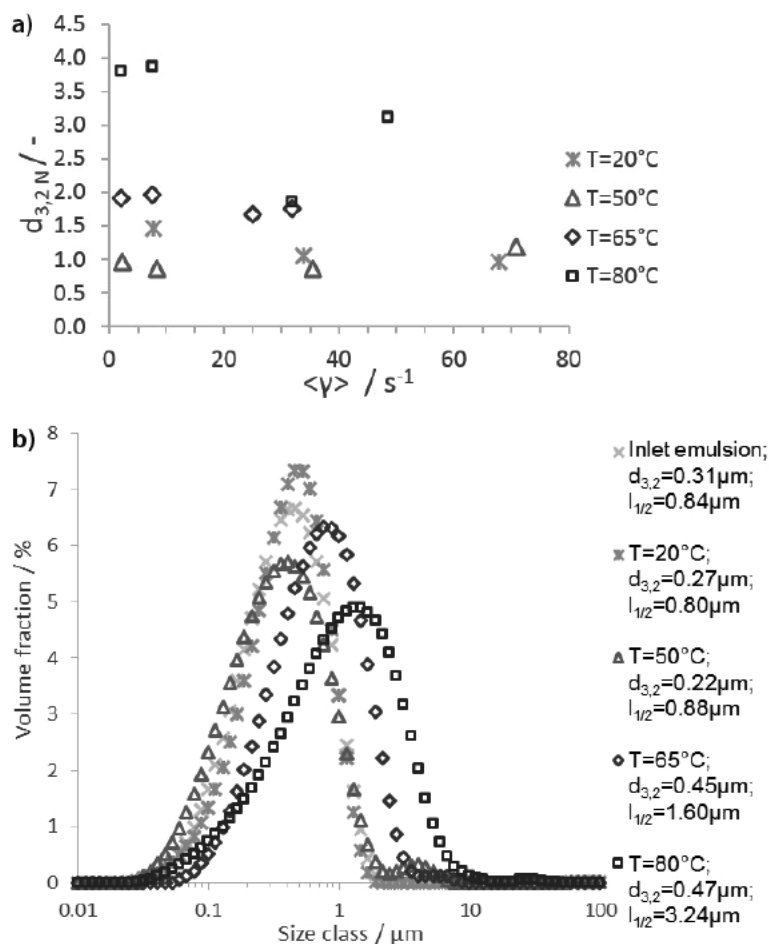


Figure 2. Influence of temperature and mean shear rate on (a) the relative Sauter mean diameter under different operating conditions and (b) the particle size distribution at the outlet of the reactor ($Q_t = 0 \text{ mL h}^{-1}$, $d = 1 \text{ mm}$, $t_r = 15 \text{ min}$).

This growth of droplets could be explained by two types of destabilization phenomena: reversible droplet aggregation and irreversible droplet growth by coalescence or Ostwald ripening. A simple experiment showed that, after 24 h of intense magnetic stirring, the drop size distribution obtained at the outlet of the reactor does not change. This would mean that the phenomena involved are irreversible, which is in agreement with the literature, where submicrometer droplets are known to limit destabilization by droplet aggregation [21]. Concerning Ostwald ripening, droplet growth is due to the Laplace pressure, which is proportional to the interfacial tension. In the present study, the interfacial tension had a constant value from 65 to $20^\circ C$, while the emulsion was more stable at $20^\circ C$ than at $65^\circ C$. Then, Ostwald ripening might not be the cause of the increase in size of the emulsion. Moreover, it has been shown for other water oil systems that an increase of the temperature implies the coalescence of droplets [22, 23] due to a decrease of the viscosity [24]. The observed evolution of the size of the emulsion might thus be explained by a coalescence phenomenon induced by the decrease in viscosity caused by the temperature increase.

Contrary to the temperature, the mean shear rate applied to the emulsion has no impact on the coalescence (Fig. 2 a) in the range of 2 80 s^{-1} . This would suggest that, under the conditions of the study, both tubing inner diameter and flow rate do not affect the structure of the emulsion, unlike high temperatures, which facilitate the coalescence of droplets.

Fig. 3 shows typical images of the emulsion at the inlet and outlet of the microchannel at $80^\circ C$ and for different flow rates. The refractive indices of the aqueous and oil phases are very similar (1.427 and 1.442, respectively). Therefore, the emulsion at the inlet looks like a homogeneous phase. Some large water drops appear at the outlet for temperatures higher than $80^\circ C$. These drops show random size, from a few micrometers to millimeters, and irregularities in frequency. They are probably formed by the coalescence of constituent parts of the dispersed phase of the emulsion.

The findings lead to the conclusion that an increase of temperature up to $50^\circ C$ induces some coalescence in the emulsion. Above $50^\circ C$, the higher the temperature, the larger the mean diameter, with increases of the initial $d_{3,2}$ by factors of 2 and 4 at 65 and $80^\circ C$, respectively. These phenomena seem to be independent of the spatial confinement and hydrodynamic conditions, i.e., of the mean shear rate.

3.2 Addition of an Aqueous Secondary Flow with Oil as Continuous Phase

The objective here was to describe the behavior of an aqueous secondary flow introduced into the tubing by using a coflow configuration when the continuous phase is oil. Experiments were performed at $20^\circ C$. In that case, the aqueous flow is dispersed and forms a drop train in the continuous organic phase.

Due to the cylindrical shape of the tubing, images showed optical distortions of drop shapes. However, they were not an issue in the present study, as the aim was just to evaluate the relative variation of the size of these drops. Consequently, it was simply assumed that drops were spherical and that there was no distortion along the axial position in the tubing. The drop length in this axis L_d was then fixed as the characteristic length of the drops.

Fig. 4 a and b respectively show the evolution of the drop sizes and the slug length, i.e., distance between two drops,

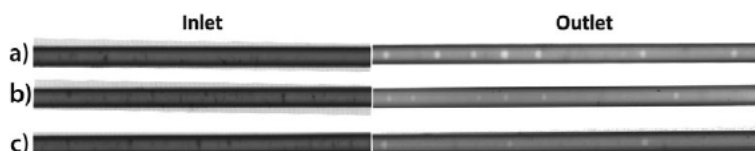


Figure 3. Emulsion at the inlet and the outlet of the microreactor ($d = 1 \text{ mm}$) at $T = 80^\circ C$ and Q_t of (a) 2 mL h^{-1} , (b) 7 mL h^{-1} at $t_r = 30 \text{ min}$, and (c) 30 mL h^{-1} at $t_r = 15 \text{ min}$.

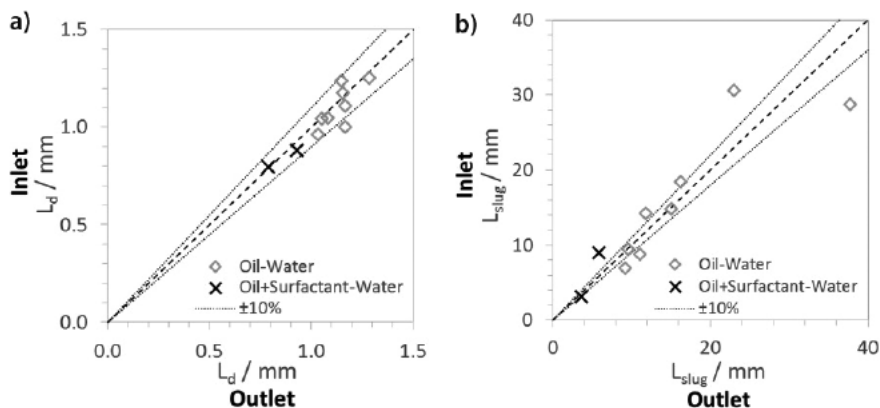


Figure 4. Comparison of (a) the drop size and (b) the slug length between the inlet and the outlet of the reactor, with and without surfactant with $d = 1$ mm and different process parameters (Q_v , Q_d/Q_c , t_r , T).

between the inlet (y axis) and the outlet (x axis) of the reactor. The presence of the surfactant leads to the formation of smaller drops (1.0–1.3 mm without surfactant vs. 0.8–1.0 mm with surfactant) and smaller L_{slug} values (10–30 mm without surfactant vs. 3 mm with surfactant). This result agrees with what could be expected, i.e., that the surfactant favors the stabilization of the drops by maximizing interfacial area and thus reducing drop size due to the decrease of the interfacial tension from 20 to less than 2 mN m^{-1} . Moreover, for all the tested conditions, the drop size and slug length are almost conserved all along the microreactor. These findings demonstrate that these two phase flows (i.e., the drop train) are hydrodynamically stable throughout the reactor.

In conclusion, it seems no breakup of the drop train occurs, even when surfactant is added at high concentration and is thus well above the critical micelle concentration. Thus, even in the presence of micelles, drops do not divide into smaller and more stable drops. At this level, it could be assumed that the behavior of the drop train will be identical when using an emulsion instead of oil, and the continuous phase of the emulsion is the standard phase studied with an excess of surfactant.

3.3 Addition of an Aqueous Secondary Flow with Emulsion as Continuous Phase

The behavior of the drop train generated by using a coflow configuration was studied with an emulsion as continuous phase. Both image analysis and measurements of the particle size distribution of the emulsion were considered.

Fig. 5 shows typical images representing the evolution of the drop train flowing through the emulsion along the microreactor at two different temperatures. Whatever the experimental conditions, two observations can be made: (1) a decrease of the drop size and (2) a trail is formed behind the drop in the emulsion

First, the decrease of the drop size along the reactor is more pronounced at

high temperature. Drops vanish after a residence time t_r of 15 min at 80°C , whereas they are still visible after a residence time of 30 min at 20°C . In parallel, a trail appears behind each drop and grows with increasing residence time. These two phenomena are concomitant. This could be explained by the fact that water contained in the drop train would diffuse towards the emulsion and lead to a local modification of the emulsion composition and of optical properties, thus drawing the observed drop trail.

To quantify the decrease in the drop size, the parameter Δ was introduced, defined by the ratio of the difference of

drop size between the inlet and the outlet of the microchannel to the drop size at the inlet (Eq. (4)):

$$\Delta = \frac{L_{d,inlet} - L_{d,outlet}}{L_{d,inlet}} \quad (4)$$

Fig. 6 illustrates the variation of this dimensionless parameter Δ with temperature for different flow rates. Depending on the operating conditions, it varies from 30 to 70 % of the initial characteristic drop size. As expected, when flow rate is higher, this phenomenon is enhanced:

For a residence time of 30 min, the decrease is between 30 and 50 % at 2 mL h^{-1} and between 40 and 60 % at 7 mL h^{-1} .

For a residence time of 15 min, the decrease is between 40 and 70 % at 30 mL h^{-1} .

The effect of temperature on the decrease in the drop size is not very pronounced below 50°C but the decrease is slightly more pronounced at high temperature especially above 50°C . In conclusion, the vanishing of drops generated by the coflow configuration and the change in droplet properties of the emulsion, observed as trails, seem to indicate that transfer of water from the drop train to the emulsion could occur. The increase of this transfer at high flow rate is probably due to better renewal of droplets at the interface of the drop train.

Regarding droplet evolution in the emulsion, Fig. 7 a and b respectively show the variation of normalized Sauter mean diameter [Eq. (3)] as a function of the mean shear rate at different temperatures and the variation of the volume size distribution of the emulsion depending on the temperature at a ratio of 10 vol % and a flow rate of 30 mL h^{-1} in a tube with 1 mm inner diameter. At 80°C , they show a strong increase of the emulsion

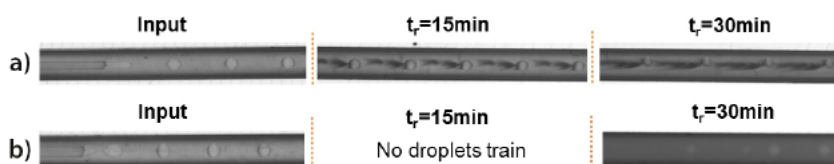


Figure 5. Visualization of the trail forming behind the drop in the emulsion and of the variation of the drop train along the reactor ($Q_t = 7 \text{ mL h}^{-1}$, $Q_d/Q_c = 5\%$) at (a) 20°C and (b) 80°C .

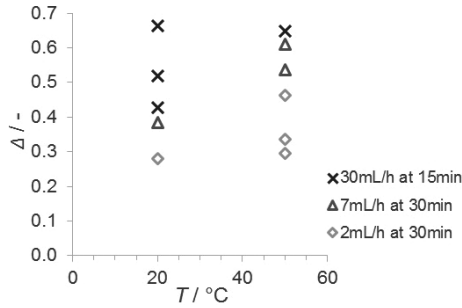


Figure 6. Normalized variation of droplets size depending on temperature and flow rate

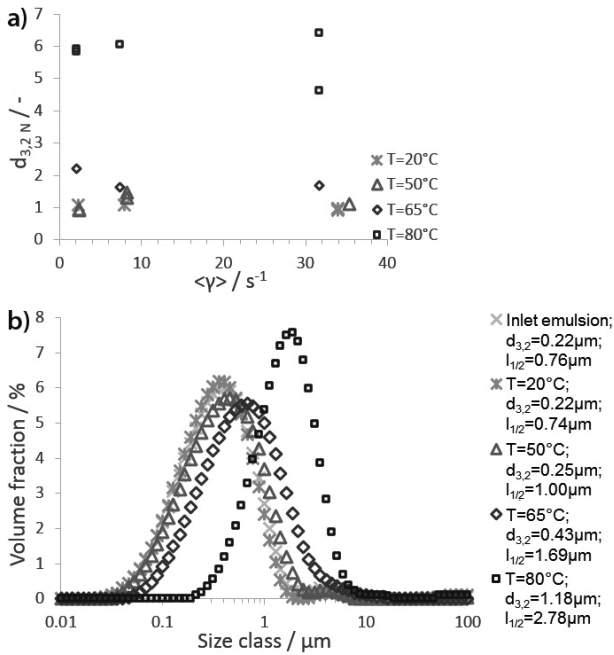


Figure 7. Influence of temperature and average shear rate on Sauter mean diameter (a) and particle size distribution of the emulsion (b) at the outlet of the reactor.

droplet size at the outlet compared to that observed at the inlet. At this temperature, multiplication of the initial $d_{3,2}$ by a factor of six, i.e., an increase of $d_{3,2}$ from 0.22 ± 0.02 to $1.18 \pm 0.04 \mu\text{m}$, is obtained. This factor of six can be compared to a factor of four under the same hydrodynamic conditions and temperature in the case of the flow of emulsion without coflow (Sect. 3.1). The coalescence is still the consequence of the high temperatures, while shear rate would have no influence on the mean diameter. Moreover, Fig. 7b shows a shift of the particle size distribution at 80°C but no broadening, contrary to case 1 (Sect. 3.1). This would suggest that all of the smallest droplets of the emulsion are involved in the increase of the characteristic size. The addition of a coflow in the microreactor would then generate new droplets in the trail of the drops, enhance the volume fraction of the dispersed phase, and contribute to the phenomenon of coalescence in the emulsion. Finally, as observed in the case in which the emulsion flows

alone in the microchannel (Fig. 3), this coalescence leads to random formation of water drops at 80°C (Fig. 5).

To further understand the phenomenon of water transfer between drop train and emulsion, clearly highlighted by the trail and drop vanishing, the effect of the volume fraction of the dispersed phase of the emulsion on the behavior of the drops was studied. Fig. 8 shows the variation of the parameter Δ with the volume fraction of dispersed phase in the emulsion at $Q_t = 7 \text{ mL h}^{-1}$, $Q_d/Q_c = 5\%$, $t_r = 15 \text{ min}$, and $T = 20^\circ\text{C}$. For identical operating conditions, the drop decrease is more important when the emulsion is more concentrated: Δ increases from 15% for the emulsion at 33 vol% of dispersed phase to 40% for the emulsion at 66 vol%. Assuming that a higher Δ means that a larger amount of water is transferred, then a high concentration of dispersed phase in the emulsion would be beneficial to the transfer between drops and droplets: when the distance between droplets and drop train is longer, i.e., the emulsion is less concentrated, the flow of water transferred would be less important. Some caution should nevertheless be taken, as, when the volume fraction of the dispersed phase of the emulsion is decreased, its apparent viscosity is lower and its particle size distribution is broader (see Appendix C). These results suggest that one of the key parameters controlling water transfer is the probability of contact between a drop of the drop train and droplets of the emulsion.

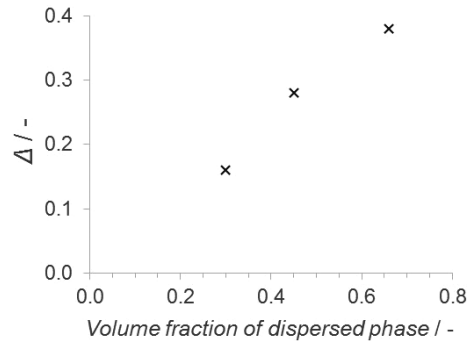


Figure 8. Influence of volume fraction of the dispersed phase on the decrease in normalized drop size Δ at $Q_t = 7 \text{ mL h}^{-1}$, $Q_d/Q_c = 5\%$ and $T = 20^\circ\text{C}$.

3.4 Discussion

At low temperature, the emulsion is not destabilized when flowing through the microreactor in the range of shear stress studied. It may be subject to destabilization when the temperature is higher than 65°C . In the system studied, coalescence may be the most likely destabilization phenomenon, promoted at high temperature when the viscosity of the system is lower.

It is possible to generate a drop train in the oil phase corresponding to the continuous phase of the emulsion in the microreactor. There is no breakup of the drop train, even when surfactant is added at high concentration, well above the critical micellar concentration.

When water drops are introduced into the emulsion, mass transfer is observed between drops and emulsion. The transfer

increases with increasing temperature and volume fraction of dispersed phase in the emulsion. According to the literature [25], a difference in osmotic pressure between the two aqueous phases (drops and droplets) could lead to a transfer of water from the more concentrated phase to the less concentrated one. In this study, two elements tend to validate this assumption:

The composition of each phase: drops of pure water and droplets of water and solutes.

The absence of transfer in the case of oil surfactant as continuous phase (Sect. 3.2).

Water migration from drops, i.e., pure water, to droplets of emulsion, i.e., water and solutes, could be then made possible. The micelles formed thanks to the excess of surfactant could act as molecule carriers for this transfer. The conservation of droplet size at 20 and 50 °C (Fig. 7) would apparently only be due to the low amount of water transferred compared to the original volume: basic calculations show indeed that it would represent a rise of less than 3 % of the Sauter mean diameter. The formation of the trail behind each drop would be induced by a slight modification of the properties of the emulsion and is localized in a small part of the emulsion visually representing around 40–50 vol % of the emulsion.

From this study, it seems now possible to implement reactive conditions involving a concentrated inverse miniemulsion. The previous results indeed enable better understanding of the phenomena involved in the present complex system and to identify the design of the microreactor and the operating domain that allows the initial properties of the concentrated inverse miniemulsion to be maintained, which is a prerequisite for implementing reactive conditions. The main characteristics for this specific system are as follows:

Spatial confinement and shear rates have no major effect on the stability of the emulsion in the studied range of operating conditions: $Q_t = 2–30 \text{ mL h}^{-1}$, $Q_d/Q_c = 2–10\%$, and $d = 0.5–1 \text{ mm}$.

The addition of a secondary flow in a coflow configuration has no effect on the stability of the emulsion as long as the temperature is lower than 65 °C.

Droplet coalescence in the emulsion can be avoided by running reactions at temperatures lower than 65 °C.

The study has shown that, in reactive systems, the transfer of reactant from the dispersed phase to the reaction site in the droplets could be possible. In microreactors, characteristic lengths are small, so mass transfer should be facilitated.

4 Conclusion

A complex multiphase system composed of a dispersed phase in a water-oil miniemulsion was implemented and studied in a microfluidic system at different temperatures. The three different configurations studied led to a better understanding of this global system involving a concentrated inverse miniemulsion. On the one hand, the study of the emulsion flowing through a microreactor showed that temperature was the key parameter influencing the stability of the emulsion. From 65 °C, droplets coalesced until the formation of new drop of water at 80 °C. On the other hand, the addition of a secondary flow in a coflow configuration flowing through a standard oil ensured the

hydrodynamic stability of the drop train. Finally, the study of water drops flowing through emulsion in a coflow configuration showed identical, but enhanced, phenomena of the emulsion but a different behavior of the drop train. Indeed water migrated from drops to droplets, probably due to a difference in osmotic pressure between these two phases and controlled by the distance between two droplets. This study has presented a framework for future work on the implementation of a reactive inverse concentrated miniemulsion in a microreactor.

Acknowledgment

We would like to acknowledge SEPPIC for their financial support and the discussions which led to progress. We also thank E. Cid for his help with image acquisition.

The authors have declared no conflict of interest.

Appendix A

Some typical rheograms of the concentrated inverse miniemulsion at different temperatures are presented in Fig. A1. A shear thinning behavior can be observed, which is affected by the temperature.

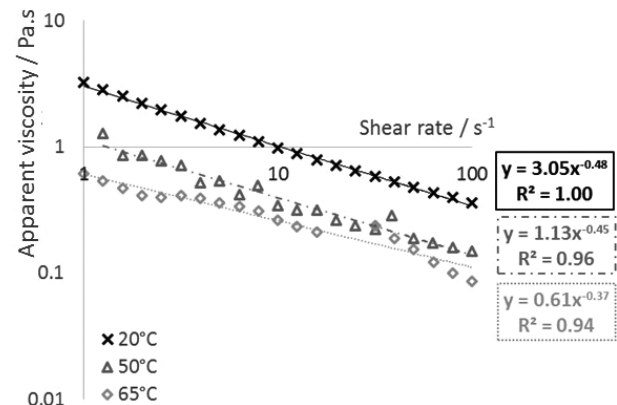


Figure A1. Rheogram of emulsions at different temperatures and power law.

Appendix B

For steady fully established laminar flows in a cylindrical tube, the axial velocity profile of shear thinning fluids described by a power law can be expressed according to [26]:

$$v_z(r) = \frac{2\tau_w}{Dk(T)} \frac{\left(\frac{D}{2}\right)^{1+\frac{1}{n(T)}} r^{1+\frac{1}{n(T)}}}{1 + \frac{1}{n(T)}} \quad (\text{B1})$$

where D is the tubing inner diameter (m) and r the radial location; k is the flow consistency index and n the flow behavior index, both of which depend on the temperature T (see Tab. 2); τ_w is the shear stress at the wall and $\dot{\gamma}_w$ the shear rate at the wall.

$$\tau_w = k(T)\dot{\gamma}_w^{n(T)} \quad (B2)$$

$$\dot{\gamma}_w = 8 \frac{v}{D} \frac{3n(T) + 1}{4n(T)} \quad (B3)$$

From Eq. (B1), the shear rate $\dot{\gamma}$ at each location r can be deduced according to:

$$\dot{\gamma}(r) = \frac{dv_z(r)}{dr} \quad (B4)$$

Then, by integrating over the channel diameter, the mean shear rate in the tube $\langle \dot{\gamma} \rangle$ can be deduced. It is reported for different operating conditions in Tab. 1.

Appendix C

Figures C1 a and b show the effect of the volume fraction of the emulsion on the viscosity at different shear rates and on the particle size distribution, respectively.

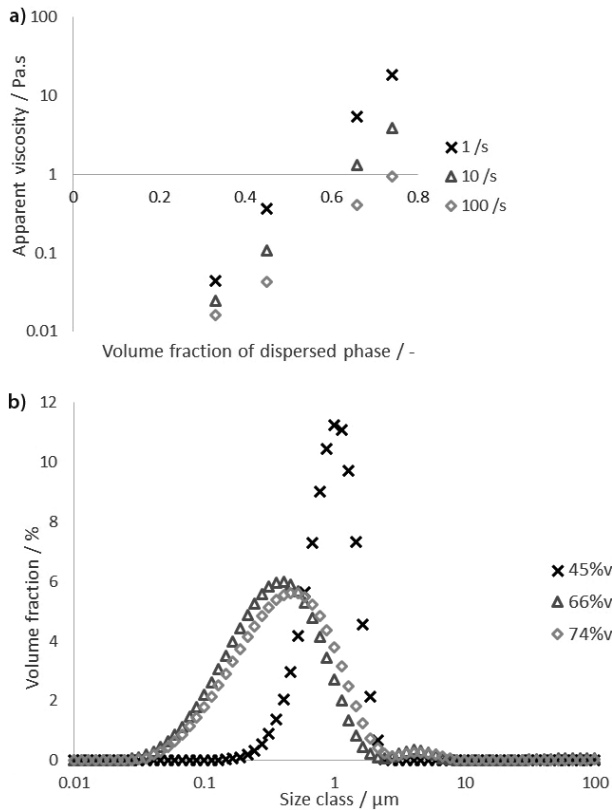


Figure C1. Evolution of viscosity (a) and particle size distribution (b) for emulsions at different volume fractions of the dispersed phase.

Symbols used

A_p	[m ²]	area of a spherical particle
D	[m]	inner diameter of the outer tubing
d	[m]	inner diameter of the inner capillary

$d_{3,2}$	[m]	Sauter mean diameter of the emulsion at the outlet of the microfluidic system
$d_{3,2i}$	[m]	Sauter mean diameter of the emulsion at the inlet of the microfluidic system
$d_{3,2N}$	[]	normalized Sauter mean diameter
$l_{1/2}$	[]	full width at half maximum
k	[kg m ⁻¹ s ⁽ⁿ⁻²⁾]	consistency
n	[]	flow index
Q_c	[m ³ s ⁻¹]	continuous phase flow rate
Q_d	[m ³ s ⁻¹]	dispersed phase flow rate
Q_t	[m ³ s ⁻¹]	total flow rate
L	[m]	length of the microreactor (i.e. the tubing)
L_d	[m]	characteristic length of a drop
L_{slug}	[m]	slug length
r	[m]	radial location
T	[K]	temperature at reactor wall
t_r	[s]	residence time
v	[m s ⁻¹]	superficial velocity
v_z	[m s ⁻¹]	axial component of the velocity in the tubing
V_p	[m ³]	volume of a spherical particle

Greek letters

Δ	[]	drop decrease ratio (Eq. (4))
$\dot{\gamma}$	[s ⁻¹]	shear rate
$\dot{\gamma}_w$	[s ⁻¹]	shear rate at the wall
$\langle \dot{\gamma} \rangle$	[s ⁻¹]	mean shear rate
τ_w	[Pa]	shear stress at the wall
μ	[Pa s]	viscosity

Abbreviations

PFA perfluoroalkoxy alkane

References

- [1] N. Kockmann, S. Karlen, C. Girard, D. M. Roberge, *Heat Transfer Eng.* **2013**, 34 (2-3), 169-177.
- [2] S. Mashaghi, A. Abbaspourrad, D. A. Weitz, A. M. van Oijen, *Trends Anal. Chem.* **2016**, 82, 118-125.
- [3] S. R. Derkach, *Adv. Colloid Interf. Sci.* **2009**, 151 (1-2), 1-23.
- [4] R. P. Borwankar, L. A. Lobo, D. T. Wasan, *Colloids Surf.* **1992**, 69 (2-3), 135-146.
- [5] B. Abismail, J. Canselier, A. M. Wilhelm, H. Delmas, C. Gourdon, *Ultrason. Sonochem.* **1999**, 6 (1-2), 75-83.
- [6] S. Maindarkar, A. Dubbelboer, J. Meuldijk, H. Hoogland, M. Henson, *Chem. Eng. Sci.* **2014**, 118, 114-125.
- [7] M. Capdevila, A. Maestro, M. Porras, J. M. Gutiérrez, *J. Colloid Interf. Sci.* **2010**, 345 (1), 27-33.
- [8] N. I. Politova, S. Tcholakova, S. Tsibranska, N. D. Denkov, K. Muelheims, *Colloids Surf. A* **2017**, 531, 32-39.
- [9] P. Mallo, G. Tabacchi (SEPPIC), *WO Patent 1999/042521*, **1999**.
- [10] M. Poux, J. P. Canselier, *Tech. Ing.* **2015**, j2152.
- [11] Tortai J. P., *Tech. Ing.* j6020 j13 V1, **2017**.

- [12] H. Karbstein, H. Schubert, *Chem. Eng. Proc.* **1995**, 34 (3), 205 211.
- [13] M. Stang, H. Schuchmann, H. Schubert, *Eng. Life Sci.* **2001**, 1 (4), 151 157.
- [14] P. D. I. Fletcher, S. J. Haswell, E. Pombo Villar, B. H. Warrington, P. Watts, S. Y. F. Wong, X. Zhang, *Tetrahedron* **2002**, 58 (24), 4735 4757.
- [15] M. Kashid, A. Renken, L. Kiwi Minsker, *Chem. Eng. J.* **2011**, 167 (2 3), 436 443.
- [16] N. Di Miceli Raimondi, L. Prat, C. Gourdon, J. Tasselli, *Chem. Eng. Sci.* **2014**, 105, 169 178.
- [17] A. A. Swinburn (Allied Colloids Limited), *EU Patent 0161038 A1*, **1985**.
- [18] O. Braun, P. Mallo, G. Tabacchi (SEPPIC), *US Patent 2003/0235547 A1*, **2003**.
- [19] O. Braun, P. Mallo, G. Tabacchi (SEPPIC), *US Patent 7943155 B2*, **2011**.
- [20] J. M. Asua, *Macromol. React. Eng.* **2016**, 10, 311 323.
- [21] T. Tadros, P. Izquierdo, J. Esquena, C. Solans, *Adv. Colloid Interface Sci.* **2004**, 108 109, 303 318.
- [22] H. Saito, K. Shinoda, *J. Colloid Interface Sci.* **1969**, 32 (4), 647 651.
- [23] B. Xu, W. Kang, X. Wang, L. Meng, *Pet. Sci. Technol.* **2013**, 31 (10), 1099 1108.
- [24] S. A. K. Jeelami, E. J. Windhab, *Chem. Eng. Sci.* **2009**, 64 (11), 2718 2722.
- [25] L. Wen, K. D. Papadopoulos, *J. Colloid Interface Sci.* **2001**, 235 (2), 398 404.
- [26] W. L. McCabe, J. C. Smith, P. Harriott, *Unit Operations of Chemical Engineering*, McGraw Hill, New York **1993**.